NMR IN BIOMEDICINE, VOL. **10**, 191–196 (1997)

Multi-Slice Perfusion-Based Functional MRI using the FAIR Technique: Comparison of CBF and BOLD effects

Seong-Gi Kim,[1]* Nikolaos V. Tsekos[1] and James Ashe[2]

[1]Center for Magnetic Resonance and Department of Radiology, University of Minnesota Medical School, 385 East River Road, Minneapolis, MN 55455, USA
[2]Brain Sciences Center, VA Medical Center, Minneapolis, MN 55417, USA

Perfusion-weighted imaging techniques employing blood water protons as an endogenous tracer have poor temporal resolution because each image should be acquired with an adequate spin 'tagging' time. Thus, perfusion-based functional magnetic resonance imaging studies are typically performed on a single slice. To alleviate this problem, a multi-slice flow-sensitive alternating inversion recovery technique has been developed. Following a single inversion pulse and a delay time, multi-slice echo-planar images are acquired sequentially without any additional inter-image delay. Thus, the temporal resolution of multi-slice FAIR is almost identical to that of single slice techniques. The theoretical background for multi-slice FAIR is described in detail. The multi-slice FAIR technique has been successfully applied to obtain three-slice cerebral blood flow based functional images during motor tasks. The relative CBF change in the contralateral motor/sensory area during unilateral thumb–digit opposition is 45.0±12.2% (n=9), while the blood oxygenation level dependent signal change is 1.5±0.4 SD%. Relative changes of the oxygen consumption rate can be estimated from CBF and BOLD changes using FAIR. The BOLD signal change is not correlated with the relative CBF increase, and thus caution should be exercised when interpreting the BOLD change as a quantitative index of the CBF change, especially in inter-subject comparisons. © 1997 John Wiley & Sons, Ltd.

NMR in Biomed. **10**, 191–196 (1997) No. of Figures: 3 No. of Tables: 1 No. of References: 34

Keywords: fMRI; cerebral blood flow; brain mapping; BOLD

Received 13 February 1997; revised 21 February 1997; accepted 21 February 1997

INTRODUCTION

The most widely used functional magnetic resonance imaging (fMRI) technique is based on the blood oxygenation level dependent (BOLD) effect,[1,2] which requires uncoupling between cerebral blood flow (CBF) and oxygen consumption changes.[3–5] However, due to the dependency on multiple parameters including CBF, oxygen consumption rate, cerebral blood volume (CBV), and vessel size, establishing a quantitative relationship between observed BOLD and physiological changes is difficult at present.[6,7] To overcome this problem, perfusion-weighted inversion recovery (IR) imaging techniques employing blood water protons as an endogenous tracer have been used.[4–8,11] In these methods, arterial blood spins tagged by means of a radio frequency (RF) pulse move into capillaries of the imaging slice and exchange with tissue water spins, providing perfusion contrast. IR methods have been successfully applied to obtain perfusion-based functional images during visual stimulation and finger and eye movements.[4,8,9,12–14]

IR-based fMRI techniques are currently implemented in a single-slice fashion.[4,8,9,12–14] Since each perfusion-weighted image requires an inversion pulse and a spin tagging time (inversion time, *TI*), the repetition time (*TR*) of a single image is on the order of seconds. Thus, the imaging time of an *N*-slice image set is $N \times TR$, reducing temporal resolution by a factor of *N*.

To improve temporal resolution, we have developed a multi-slice flow-sensitive alternating inversion recovery (FAIR) technique to acquire multi-slice perfusion-weighted images, with a temporal resolution almost identical to that of a single slice image (temporal resolution=TR). Furthermore, with this approach, the signal-to-noise ratio per time required to obtain a multi-slice data set increases. Following a single inversion pulse and *TI*, multi-slice echo-planar images are acquired sequentially without any additional inter-image delay. Since each image can be collected in 50 ms, the imaging time for three slices is the sum of *TI* and 0.15 s. The multi-slice FAIR technique was successfully applied to obtain three-slice perfusion-weighted functional images during motor tasks. Since nonslice selective IR images contain signal contributions from the BOLD effect, the relative change of oxygen consumption rate was estimated from CBF and BOLD fractional signal changes, employing various assumptions (e.g. CBV and oxygenation level).[6,7]

* Correspondence to: Seong-Gi Kim, CMRR, University of Minnesota Medical School, 385 East River Road, Minneapolis, MN 55455, USA. E-mail: kim@geronimo.drad.umm.edu.
Contract grant sponsor: National Institutes of Health; *contract grant number:* RR08079; *contract grant number:* MH57180; *contract grant number:* NS32919
Contract grant sponsor: Whitaker Foundation.
Contract grant sponsor: University of Minnesota.

© 1997 John Wiley & Sons, Ltd. CCC 0952–3480/97/040191–06 $17.50

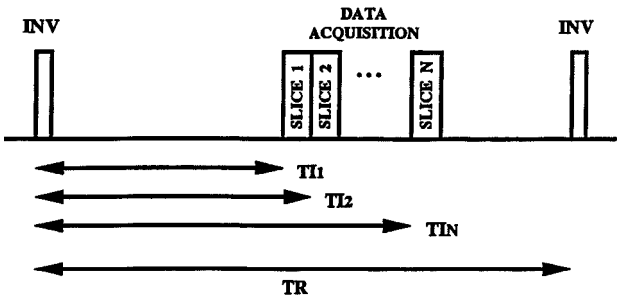

Figure 1. A multi-slice FAIR scheme. Following inversion (INV), images are acquired sequentially from the first slice (SLICE 1) to the *N*th slice (SLICE *N*) without any additional inter-image delay. TI_1, TI_2 and TI_N represent inversion times of slices 1, 2 and *N*, respectively. *TR* represents the repetition time.

TECHNIQUES AND THEORY

Two IR images in each slice are acquired by the multi-slice FAIR technique; one with a slice-selective inversion pulse, and the other with a nonslice selective inversion pulse. Multi-slice images are obtained after an inversion pulse and a subsequent tagging delay t (i.e. TI) (see Fig. 1). The magnetization of tissue spins at t is denoted as $M(t)$ and the magnetization of arterial blood spins at t is $M_a(t)$. In slice selective IR (ssIR), $M_a(t)$ outside the inversion slab is the relaxed longitudinal magnetization M_o; $M(0)$ within the inversion slab is $-M_o$. In single-sliced FAIR studies, the distance between the inferior edge of the imaging slice and the superior edge of the slice-selective inversion slab is short (e.g. 5 mm), and the delivery of tagged spins is almost instantaneous. However, in multislice studies, the delivery times Δ of tagged spins into the imaging slice differ and should be considered. Prior to Δ, inverted arterial spins within the inversion slab are relaxed by T_1; $M_a(t)$ is $M_o\,(1-2\cdot\exp(-t/T_1))$ when $t \leq \Delta$, and M_o when $t > \Delta$. Thus, $M(t)$ recovers with T_1 when $t \leq \Delta$, and later with the apparent longitudinal relaxation time $T_1^\star$ which contains an inflow component, i.e. $1/T_1^\star = 1/T_1 + f/\lambda$ where f is the CBF (ml/g tissue/s) and λ is the tissue-to-blood partition coefficient. For simplicity, we assume that both tissue and blood have the same T_1. The longitudinal magnetization of ssIR images at the inversion time of TI, $M_{ss}(TI)$, is then

$$M_{ss}(TI) = \begin{cases} M_o - 2\cdot M_o \cdot e^{-TI/T_1} & TI \leq \Delta \\ M_o - 2\cdot M_o \cdot e^{-(TI-\Delta)\cdot \frac{f}{\lambda}} \cdot e^{-TI/T_1} & TI > \Delta \end{cases} \quad (1)$$

In nonslice selective IR (nsIR), $M_a(0)$ and $M(0)$ are inverted. When spins in the whole body are inverted for nsIR, $M_a(t)$ relaxes with T_1 during the entire tagging time. However, when a head coil or a surface coil is used, nonslice selective inversion affects only a limited volume, and thus fully relaxed untagged spins may arrive at time τ. $M_a(t)$ will be M_o–$2M_o \cdot \exp(-t/T_1)$ when $t \leq \tau$, and M_o when $t > \tau$. The longitudinal magnetization of nsIR images at the inversion time TI, $M_{ns}(TI)$, is

$$M_{ns}(TI) = \begin{cases} M_o - 2\cdot M_o \cdot e^{-TI/T_1} & TI \leq \tau \\ M_o - \cdot M_o \cdot e^{-(TI-\tau)\cdot \frac{f}{\lambda}} \cdot e^{-TI/T_1} & TI > \tau \end{cases} \quad (2)$$

The FAIR signal S_{FAIR} is the difference between ssIR and nsIR signal intensities. Thus, the subtraction of eq. (2) from eq. (1) will leave

$$S_{FAIR} = \Delta M(TI) = \begin{cases} 0 & TI \leq \Delta \\ 2M_o \cdot e^{-TI/T_1} \cdot (TI-\Delta)\cdot f/\lambda & \Delta < TI \leq \tau \\ 2M_o \cdot e^{-TI/T_1} \cdot (\tau-\Delta)\cdot f/\lambda & TI > \tau. \end{cases} \quad (3)$$

For the measurement of CBF from multi-slice FAIR images using eq. (3), transit times Δ and τ, M_o and T_1 need to be determined. When T_1 and $T_1^\star$ are determined individually using data acquired with TIs ranging between Δ and τ, f can be directly determined without concerning the delivery time of tagged spins. In the case that blood T_1 (T_{1a}) is not same as tissue T_1, eq. (3) needs to be modified with the correction factor $K(\tau-\Delta, T_1, T_{1a})$ when $TI > \tau$ or $K(TI-\Delta, T_1, T_{1a})$ otherwise, which is $K(t, T_1, T_{1a}) = [1-\exp(-\gamma t)]/\gamma t$ where $\gamma = 1/T_{1a} - 1/T_1$.[10, 11, 15–17]

In fMRI studies, FAIR images are acquired repeatedly during both control and stimulation periods, and their average signal intensities, $S_{FAIR(cont)}$ and $S_{FAIR(st)}$, are obtained during both periods. The relative signal changed during the task period is described by

$$\frac{S_{FAIR(st)}}{S_{FAIR(cont)}} = \begin{cases} \dfrac{TI-\Delta_{st}}{TI-\Delta_{cont}} \cdot \dfrac{f_{st}}{f_{cont}} & \Delta_{cont} \leq TI < \tau_{cont} \\ \dfrac{\tau_{st}-\Delta_{st}}{\tau_{cont}-\Delta_{cont}} \cdot \dfrac{f_{st}}{f_{cont}} & TI \geq \tau_{cont} \end{cases} \quad (4)$$

where Δ_{cont} and Δ_{st} are the delivery times of tagged spins into the imaging slice from outside the slice-selective inversion slab in ssIR during control and stimulation periods, respectively, and τ_{cont} and τ_{st} are the transit times of untagged spins into the imaging slice in nsIR. Most importantly, T_1 of tissue and blood do not play a role since we do not expect changes in T_1 during the stimulation period. When $\Delta \approx 0$, e.g. in the single-slice FAIR image, and $TI < \tau$, relative CBF (relCBF) changes can be directly determined from the relative signal changes in FAIR.[9, 14] Task-induced neuronal activity causes an increase in arterial blood velocity, decreasing both Δ and τ. If TI is shorter than τ with a significant Δ value, relCBF determined without consideraiton of Δ is overestimated. For the case in which the magnitude of changes in Δ and τ is similar during the stimulation period and $TI > \tau$, relCBF is equivalent to the relative change in the FAIR signal. Thus, it is important to have an inversion time which is longer than τ to minimize errors in the determination of relCBF. For example, in cases where Δ_{st} and Δ_{cont} are 0.3 and 0.5 s, and τ_{st} and τ_{cont} are 1.0 and 1.2 s, respectively,[15] the error of not considering transit times is negligible when $TI > 1.2$ s. In this study, we assume that $\tau_{st} - \Delta_{st}$ equals $\tau_{cont} - \Delta_{cont}$.

Due to the use of echo planar imaging (EPI) data collection in multi-slice FAIR, $T_2^\star$ contribution to the IR images is inevitable. BOLD percent changes obtained from nsIR images can be used for two purposes; one is to eliminate the BOLD effect in calculations of relCBF changes, and the other is to estimate oxygen consumption changes with various assumptions. From the FAIR and nsIR signal changes, the relative FAIR signal change due only to flow can be calculated as (1 + fractional change of FAIR)/(1 + fractional change of nsIR) − 1.[9]

Changes of venous oxygenation levels, $\Delta Y/(1-Y)$, can be determined from BOLD signal changes of nsIR. According to Ogawa *et al.*,[6, 18] fractional signal changes,

© 1997 John Wiley & Sons, Ltd.

$\Delta S/S$, of BOLD images can be described as

$$\frac{\Delta S}{S} = A \cdot TE \cdot (1 - Y) \cdot \mathrm{b} \cdot \left(\frac{\Delta Y}{1 - Y} - \frac{\Delta b}{b} \right) \qquad (5)$$

where A is a constant, TE is the gradient echo time, Y is the venous blood oxygenation level during the resting condition, and b is the venous blood volume. The constant A depends on many parameters including the main magentic field, the vessel orientation, and the susceptibility difference between 100% deoxygenated blood and 100% oxygenated blood. Based on simulations with static averaging for low resolution images where the voxel contains many vessels with various orientations, A is 510 at 4 T.[18] Y is set to 0.54.[19] We assume that $b = 0.03$. The capillary volume fraction of cat brain is $2.1 \pm 0.5\%$,[20] and the average CBV values of monkey brain, determined by X-ray fluorescence and positron emission tomography (PET) are 4.7 and 3.5 ml/100 g tissue, respectively.[21,22] Since we expect BOLD signal changes at all venous vessels including capillaries, the value used here is larger than the capillary volume and smaller than the total blood volume. The relative blood volume change, $\Delta b/b$, is closely related to the CBF change; we assume that, according to PET studies,[22] $\Delta b/b = (\Delta CBF/CBF + 1)^{0.38} - 1$ where $\Delta CBF/CBF$ is the relative CBF change. Using the conservation of matter (Fick's principle), the relative change of cerebral metabolic rate of O_2 ($CMRO_2$; oxygen consumption rate) in tissue, $relCMRO_2$, can be determined from the relative changes of both CBF and oxygenation level in venous vessels. Their relationship is $relCMRO_2 = (\Delta CBF/CBF + 1)(1 - \Delta Y/(1 - Y)) - 1$. With both relCBF obtained from FAIR and $\Delta Y/(1 - Y)$ estimated using eq. (5), $relCMRO_2$ can be determined.

METHODS AND MATERIALS

Normal human subjects were studied on a 4 T whole body imaging system with a 1.25 m diameter horizontal bore (SISCo., Palo Alto, CA/Siemens, Erlangen, Germany) and a head gradient insert operating at gradient strength of 30 mT/m and a slew rate of 150 T/m/s in all three axes. For RF transmission and detection, a homogeneous quadrature coil (length = 22 cm, inner diameter = 26.5 cm) was used.[23] To improve field homogeneity, either a field mapping technique[24] or manual shimming was used.

Prior to functional imaging studies, T_1-weighted images were acquired using an interleaved EPI technique.[25] The parameters were a TI of 1.2 s, an echo time (TE) of 8 ms, an in-plane resolution of 1.88×1.88 mm^2, and a slice thickness of 5 mm. In addition, conventional anatomic images were collected using a turbofast low angle shot (TurboFLASH) technique.[26] Typical imaging parameters were a TI of 1.2 s, a TE of 4.7 ms, a TR of 9.6 ms, and an in-plane resolution of 0.94×0.94 mm^2.

The multi-slice FAIR scheme was implemented using two IR images with and without slice-selective gradients during an inversion pulse in an interleaved fashion. The inversion pulses were hyperbolic secant pulses with a pulse length of 8 ms.[27] After the inversion pulse and TI, multi-slice EPI images were acquired sequentially without any additional inter-image delay, as illustrated in Fig. 1. A single-shot blipped EPI technique was implemented with trapezoidal gradient shapes for the readout and blipped gradients for the phase-encoding direction. The axial EPI images had a 64×64 matrix size over a field of view of 24×24 cm^2 with 5 mm slice thickness. The gradient echo time was 20 ms, the acquisition time was 30 ms, and the imaging time for a single slice was 50 ms. A five-lobe sinc-shaped 90° RF pulse with 4 ms duration was used for the excitation of spins. *Three-slice* FAIR images were collected from the superior to the inferior slice. Inversion times for the first, second and third imaging slices were 1.4, 1.45 and 1.5 s, respectively. The inversion times are close to T_1 of gray matter water at 4 T,[28] providing maximal FAIR sensitivity.[9] The time between the excitation pulse of the first slice and the subsequent inversion pulse was typically 1.55 s. The TR was 2.95 s for three-slice IR images. A 15 mm-thick slab was used for FAIR images, and the thickness of the slice-selective inversion slab was 25 mm, which is larger than the FAIR slice thickness to minimize perturbation of the magnetization due to imperfect RF pulses.

In sequential acquisition of multi-slice EPI images without any additional inter-image delay, the excitation pulse for one slice may affect the magnetization of subsequently acquired neighboring slices. To determine edge effects of excitation pulses, EPI images of the middle slice were acquired under three different conditions: (i) without applying any pulses in neighbouring slices (i.e. a spin density image), (ii) after excitation of one neighboring slice, and (iii) after excitation of both neighboring slices. The signal intensity of the whole slice was obtained and normalized to the spin density.

The multi-slice FAIR technique was applied to fMRI studies. Slices were selected axially through the motor cortex area. Image sets were collected repeatedly during control and task periods. Usually, 15 image sets were acquired during each period. The task was auditory-cued unilateral finger opposition of the thumb and the other four digits. The frequency of instruction for movements was 1.0 Hz.

K-space data were zero-filled to 128×128, line-broadened by a gaussian function with a full-width at half-maximum of $0.7 \times$ pixels, and then Fourier-transformed. All FAIR images were generated by pairwise subtraction of the nsIR image from the ssIR image in magnitude mode. From consecutive images generated during the paradigm, functional maps were calculated according to two criteria: (i) A cross-correlation method was used with a boxcar reference waveform;[29] only pixels with a statistically significant activation ($p < 0.05$) were included. The cross-correlation value was chosen, based on the number of images used.[29] (ii) Since zero-filling and line-broadening were used, regions with less than eight contiguous activated in-plane pixels were not included in the functional map.[30]

Activated pixels were determined from FAIR functional maps. To calculate the average fractional signal change of FAIR and BOLD in each study, the average signal intensity of *activated pixels* within the contralateral motor/sensory area was obtained during control and task periods. Then the average signal difference between control and task conditions was divided by the signal intensity during the control periods. Relative CBF changes were calculated from FAIR relative signal changes by taking into account BOLD effects of nsIR (see Theory section). $\Delta Y/(1 - Y)$ and $relCMRO_2$ were calculated using eq. (5). Statistical analyses for comparisons of different measurements were performed.

© 1997 John Wiley & Sons, Ltd.

RESULTS

To study edge effects of neighboring slices caused by RF pulses, five subjects were studied. The signal intensity of the image acquired 50 ms after excitation of one neighboring slice was 1.009 ± 0.018 of the spin density image, and that acquired 50 ms after one slice excitation and 100 ms after the other slice excitation was 1.018 ± 0.027 of the spin density image. Thus, perturbation of the magnetization in neighboring slices caused by RF pulses is minimal, and was therefore not corrected for further studies.

Plate 1 shows three-slice FAIR images (A) and corresponding functional maps (B–D) overlaid on T_1-weighted EPI images of one representative subject (no. 1L) during left-hand finger opposition. In the FAIR images (A), white and gray matter contrast is excellent; white matter appears dark, while gray matter appears bright because of its higher CBF. Large vessel areas appear bright due to complete replenishment by fresh spins. Fast flow in such vessels causes flow artifacts in the phase-encoding direction in EPI. The resulting artifacts in the FAIR images are evident, for example in the sagittal sinus region.

Percent signal changes were calculated only in statistically significant pixels. Functional maps B, C and D are based on FAIR, ssIR and nsIR, respectively. Arrows indicate the right central sulcus; the motor cortex is located anterior to the central sulcus. During left-hand finger opposition, the right motor area was activated in all functional images. In FAIR functional maps, CBF changes were on the order of 50% in tissue areas. Percent signal changes were similar in all three slices. Furthermore, small but significant activation in ipsilateral (left) motor cortex and bilateral supplementary motor area (i.e. medial area) was seen. In nsIR and ssIR functional maps, large signal changes (i.e. 10%) were observed at the edge of the brain, while tissue areas had 1–3% changes. Note that the area indicated by the arrow at the edge of the brain in the middle slice had large percent changes (shown in red) in ssIR and nsIR, but not in FAIR. This area is located at a draining Rolandic vein, remote from neuronally active areas, which have a large BOLD effect.

Nine experiments (six right-handed subjects) were performed during unilateral finger opposition at a frequency of 1.0 Hz. In all studies, contralateral motor/sensory and bilateral supplementary motor areas were consistently activated. In some subjects, the ipsilateral motor area was activated as well. Relative CBF and BOLD signal changes in the contralateral motor/sensory area are tabulated in Table 1, and relative CBV, venous oxygenation and relative $CMRO_2$ changes computed from relCBF and BOLD values are also shown. The average activation area in the contralateral motor/sensory area is 5.3 ± 1.0 SD cm^3, and the average relCBF change is 45.0 ± 12.2 SD % ($n = 9$), ranging from 30.1 to 68.7%. The relCBF values obtained using multi-slice FAIR agree well with the values measured by single-slice FAIR techniques.[9,14] The average BOLD percent signal change with a *TE* of 20 ms is 1.5%. Figure 2

Table 1. Percent changes of CBF, BOLD, cerebral blood volume (CBV), venous oxygenation level ($\Delta Y/(1\text{-}Y)$) and oxygen consumption ($relCMRO_2$) in the contralateral motor/sensory area during finger opposition[1]

Subject	Volume (cm^3)	relCBF	BOLD	CBV	$\Delta Y/(1\text{-}Y)$	$relCMRO_2$
1L	8.6	50.0	0.9	16.6	23.0	15.4
1R	5.5	30.1	1.1	10.5	18.3	6.2
2L	5.2	49.6	0.8	16.5	22.2	16.4
2R	3.3	53.3	1.9	17.6	31.1	5.6
3L	5.0	68.7	1.4	22.0	32.2	14.4
3R	4.5	43.4	2.2	14.7	30.2	0.0
4L	4.7	31.1	1.6	10.8	22.5	1.6
5L	4.1	44.5	1.7	15.0	27.1	5.4
6L	7.0	34.0	1.6	11.8	23.3	2.8
Mean ± SD	5.3 ± 1.0	45.0 ± 12.2	1.5 ± 0.4	15.1 ± 3.6	25.5 ± 4.7	7.5 ± 5.5

[a] Six subjects performed sequential thumb-digit opposition using the right (R) or left (L) hand. All activated pixels ($p < 0.05$) in the FAIR images within the motor/sensory area contralateral to the moving limb were used. Relative CBF changes were obtained from FAIR percent signal changes by taking into account the BOLD contribution, and BOLD signal changes with *TE* of 20 ms were from nonslice selective IR images. Calculations of CBV, $\Delta Y/(1\text{-}Y)$ and $relCMRO_2$ were shown in the text.

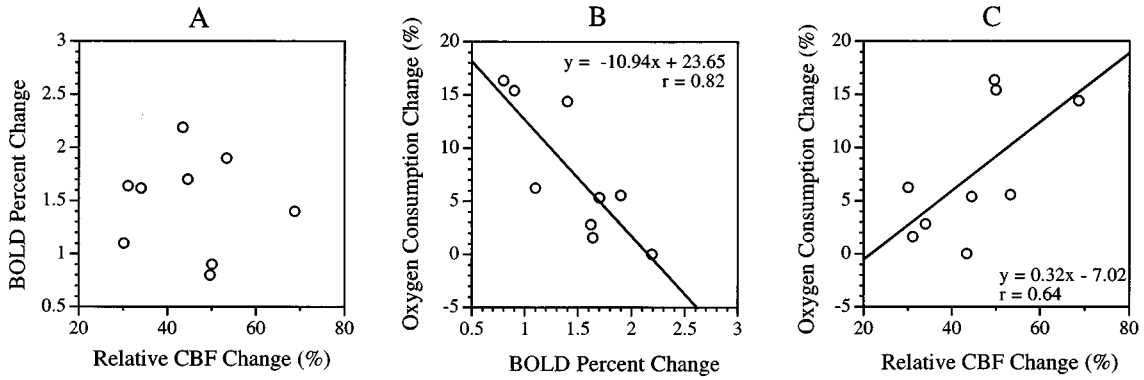

Figure 2. Relationships of the mean changes of the CBF, BOLD and $CMRO_2$. Nine data points from six subjects were used. BOLD fractional signal changes were obtained from nsIR images with the gradient echo time of 20 ms. (A) represents the relation between relCBF and BOLD changes; (B) the relationship between BOLD and $relCMRO_2$ changes; and (C) the relationship between CBF and $relCMRO_2$ changes. Fitted equations and *r* values are shown.

© 1997 John Wiley & Sons, Ltd.

shows the relationships of relCBF, BOLD and relCMRO$_2$ changes. The correlation coefficients (cc) calculated across all nine measurements were -0.83 between BOLD and relCMRO$_2$, and 0.64 between relCBF and relCMRO$_2$. No correlation was found between relCBF and BOLD ($cc = 0.08$).

DISCUSSION

An important consideration for multi-slice FAIR imaging is the delivery of tagged spins into the blood arterial system of the imaging slices. There are two components for spin delivery into the imaging slice; one is by large and small arteries and the other is by arterioles and capillaries. Since the length of arterioles and capillaries is less than 1 mm[31] and hence less than the voxel dimension used in this study, their spin delivery will be similar in all imaging slices. The spin delivery by large and small arteries is dependent on both travel distance of tagged spins and arterial blood velocity. Arterial blood velocity is ≥ 10 cm/s.[32] Assuming the orientation of these vessels to be perpendicular to the imaging slice, it takes ≤ 250 ms (Δ) for tagged spins to traverse a 2.5 cm slice-selective inversion slab. Another important issue is the time τ for the untagged spins in nsIR to move into the imaging slice. For cases in which the distance between the neck and the imaging slab is approximately 15 cm, τ is less than 1.5 s. During increased CBF, Δ and τ decrease at the same time, and thus relCBF values determined here have minimal errors.

In principle, multi-slice FAIR imaging can be extended to cover the whole brain during an fMRI study. For example, 15 axial slices covering the entire brain can be collected within 600 ms because each slice can be acquired within 40 ms using single-shot EPI. This implementation requires that, in the nonslice selective IR images, all spins entering the imaging slice during *TI* experience inversion. In the present study, a homogeneous head coil was used in which the nonslice selective inversion pulse inverts spins in the brain but not in the neck and heart. In cases in which the imaging slab is close to the inferior side of the nonslice selective inversion slab, such as the cerebellum, untagged spins in the neck may travel into the imaging slice during *TI* (i.e. $TI > \tau$). This causes reduction of signal intensity in FAIR images (see eq. (4)). To minimize this problem, a body coil can be used for inversion, allowing for spin tagging of the neck and possibly the heart for nonslice selective IR; for the accurate determination of relCBF from FAIR signal changes in fMRI studies, transit times Δ of tagged spins should be measured and corrected (eq. (4)).

Since nsIR images acquired as part of FAIR contain the BOLD effect with gradient echo times of 20 ms, relative venous oxygenation level and oxygen consumption changes can be computed with various assumptions. Oxygenation level change ($\Delta Y/(1-Y)$) in the motor/sensory area, 26 ± 6 SD% ($n = 9$) agrees well with that in pial veins within the motor cortex during finger opposition, 30%.[33] The relative oxygen consumption rate change is $\sim 8\%$ during finger opposition, which is higher than that during visual stimulation, 5%, calculated from BOLD and FAIR with the same assumptions.[34]

Nonetheless, determination of oxygenation level and oxygen consumption changes from BOLD and FAIR should be validated. A hypercapnia model can be used, in which CBF increases without any oxygen consumption change.

In this study, the BOLD signal change is not correlated to the relative CBF change *across measurements*. This may be related to anatomical and physiologial differences including vessel architectures, venous oxygenation levels and oxygen consumption. Interestingly, the calculated oxygen consumption rate is weakly correlated with the CBF change within the motor/sensory area during finger opposition *across measurements*; however, it is not clear whether this observation is related to anatomical (vasculature) or physiological differences (oxygen consumption) between subjects. Further investigations are needed to determine the relationship between CBF and BOLD changes by measuring them in the same subject during different tasks.

Clearly, the BOLD signal change is negatively correlated with the relCMRO$_2$. Similar correlation was also observed during visual stimulation.[34] This can be expected because BOLD is based on uncoupling between CBF and relCMRO$_2$. At a given relCBF, the higher the oxygen consumption rate, the less BOLD signal change will be obtained. Thus, higher BOLD changes do not necessarily mean higher CBF changes. Caution should be exercised when interpreting the BOLD percentage change as a quantitative index of the CBF change, especially in inter-subject comparisons.

CONCLUSION

A multi-slice FAIR technique, using a single inversion pulse for all slices, has been developed and successfully applied to obtain CBF-based functional maps during motor tasks. Multi-slice FAIR was demonstrated with three slices in this study, but more slices can be obtained. In the multi-slice FAIR-based fMRI techniques, changes of the BOLD effect in nsIR images and the CBF effect in FAIR images can be used to calculate the oxygen consumption change. The BOLD signal change is not correlated with the CBF change across subjects, while the BOLD change is negatively correlated with relCMRO$_2$.

Acknowledgements

The authors thank Peter Andersen and Gregor Adriany for hardware support, and John Strupp for his processing software (STIMULATE). Supported by NIH grants RR08079, MH57180, NS32919 and NS32437, a Whitaker Foundation grant and a Grant-in-Aid from the University of Minnesota.

REFERENCES

1. Ogawa, S., Lee, L.-M., Nayak, A. S. and Glynn, P. Oxygenation-sensitive contrast in magnetic resonance imaging of rodent brain at high magnetic fields. *Magn. Reson. Med.* **14**, 68–78 (1990).
2. Ogawa, S., Lee, T.-M., Kay, A. R. and Tank, D. W. Brain magnetic resonance imaging with contrast dependent on blood oxygenation. *Proc. Natl Acad. Sci. USA* **87**, 9868–9872 (1990).
3. Ogawa, S., Tank, D. W., Menon, R. S., Ellermann, J. M., Kim, S.-G., Merkle, H. and Ugurbil, K. Intrinsic signal changes

© 1997 John Wiley & Sons, Ltd.

accompanying sensory stimulation: functional brain mapping using MRI. *Proc. Natl Acad. Sci. USA* **89**, 5951–5955 (1992).
4. Kwong, K. K., Belliveau, J. W., Chesler, D. A., Goldberg, I. E., Weisskoff, R. M., Poncelot, B. P., Kennedy, D. N., Hoppel, B. E., Cohen, M. S., Turner, R., Cheng, H.-M., Brady, T. J. and Rosen, B. R. Dynamic magnetic resonance imaging of human brain activity during primary sensory stimulation. *Proc. Natl Acad. Sci. USA* **89**, 5675–5679 (1992).
5. Bandettini, P. A., Wong, E. C., Hinks, R. S., Tifofsky, R. S. and Hyde, J. S. Time course EPI of human brain function during task activation. *Magn. Reson. Med.* **25**, 390–397 (1992).
6. Ogawa, S., Menon, R. S., Tank, D. W., Kim, S.-G., Merkle, H., Ellermann, J. M. and Ugurbil, K. Functional brain mapping by blood oxygenation level-dependent contrast magnetic resonance imaging. *Biophys. J.* **64**, 803–812 (1993).
7. Weisskoff, R. M., Zuo, C. S., Boxerman, J. L. and Rosen, B. R. Microscopic susceptibility variation and transverse relaxation: theory and experiment. *Magn. Reson. Med.* **31**, 601–610 (1994).
8. Edelmann, R. R., Siewert, B., Darby, D. G., Thangaraj, V., Nobre, A. C., Mesulam, M. M. and Warach, S. Qualitative mapping of cerebral blood flow and functional localization with echo-planar MR imaging and signal targeting with alternating radio frequency. *Radiology* **192**, 513–520 (1994).
9. Kim, S.-G. Quantification of relative blood flow change by flow-sensitive alternating inversion recovery (FAIR) technique: application to functional mapping. *Magn. Reson. Med.* **34**, 293–301 (1995).
10. Kwong, K. K., Chesler, D. A., Weisskoff, R. M., Donahue, K. M., Davis, T. L., Ostergaard, L., Campbell, T. A. and Rosen, B. R. MR perfusion studies with T_1-weighted echo planar imaging. *Magn. Reson. Med.* **34**, 878–887 (1995).
11. Schwarzbauer, C., Morrissey, S. P. and Haase, A. Quantitative magnetic resonance imaging of perfusion using magnetic labeling of water proton spins within the detection slice. *Magn. Reson. Med.* **35**, 540–546 (1996).
12. Sane, J. N., Donoghue, J. P., Thangaraj, V., Edelman, R. R. and Warach, S. Shared neural substrates controlling hand movements in human motor cortex. *Science* **268**, 1775–1777 (1995).
13. Darby, D. G., Nobre, A. C., Thangaraj, V., Edelmann, R. R., Mesulam, M. M. and Warach, S. Cortical activation in the human brain during lateral saccades using EPISTAR functional magnetic resonance imaging. *Neuroimage* **3**, 53–63 (1996).
14. Kim, S.-G. and Tsekos, N. V. Perfusion imaging by a flow-sensitive alternating inversion recovery (FAIR) technique: application to functional brain imaging. *Magn. Reson. Med.* **37**, 425–435 (1997).
15. R. B. Buxton, L. R. Frank, B. Siewert, S. Warach and R. R. Edelman. A quantitative model for a EPISTAR perfusion imaging. *Proceedings of the 3rd Meeting of the Society of Magnetic Resonance*, p. 132 (1995).
16. Buxton, R. B., Wong, E. C. and Frank, L. R. Quantitation issues in perfusion measurement with dynamic arterial spin labeling. *Proceedings of the 4th Meeting of the Society of Magnetic Resonance*, p. 10 (1996).
17. Calamante, F., Williams, S. R., van Bruggen, N., Kwong, K. K. and Turner, R. A model of quantification of perfusion in pulsed labelling techniques. *NMR Biomed.* **8**, 79–84 (1996).
18. Ogawa, S., Lee, T.-M. and Barrere, B. The sensitivity of magnetic resonance imaging signals of a rat brain to changes in the cerebral venous blood oxygenation. *Magn. Reson. Med.* **29**, 205–210 (1993).
19. Lai, S., Haacke, E. M., Lin, W., Chien, D. and Levin, D. *In vivo* measurement of cerebral blood oxygenation with MRI. *Proceedings of the 3rd Meeting of the Society of Magnetic Resonance*, p. 849 (1995).
20. Pawlik, G., Rackl, A. and Bing, R. J. Quantitative capillary topography and blood flow in the cerebral cortex of cats: an *in vivo* microscopic study. *Brain Res.* **208**, 35–58 (1981).
21. Phelps, M. E., Grubb, Jr., R. L. and Ter-Pogossian, M. M. Correlation between $PaCO_2$ and regional blood volume by X-ray fluoroscence. *J. Appl. Physiol.* **35**, 447–475 (1973).
22. Grubb, Jr., R. L., Raichle, M. E., Eichling, J. O. and Ter-Pogossian, M. M. The effects of changes in $PaCO_2$ on cerebral blood volume, blood flow, and vascular mean transit time. *Stroke* **5**, 630–639 (1974).
23. Adriany, G., Vaughan, J. T., Andersen, P., Merkle, H., Garwood, M. and Ugurbil, K. Comparison between head volume coils at high fields. *Proceedings of the 3rd Meeting of the Society of Magnetic Resonance*, p. 747 (1995).
24. Gruetter, R. Automatic, localized *in vivo* adjustment of all first- and second-order shim coils. *Magn. Reson. Med.* **29**, 804–811 (1993).
25. Kim, S.-G., Hu, X., Adriany, G. and Ugurbil, K. Fast interleaved echo-planar imaging with navigator: high resolution anatomic and functional images at 4 Tesla. *Magn. Reson. Med.* **35**, 895–902 (1996).
26. Haase, A. Snapshot FLASH MRI: application to T_1, T_2- and chemical shift imaging. *Magn. Reson. Med.* **13**, 77–89 (1990).
27. Garwood, M. and Ugurbil, K. B_1 Insensitive adiabatic pulses. *NMR Basic Principles Progress* **26**, 110–147 (1992).
28. Kim, S.-G., Hu, X. and Ugurbil, K. Accurate T_1 determination from inversion recovery images: application to human brain at 4 Tesla. *Magn. Reson. Med.* **31**, 445–449 (1994).
29. Bandettini, P. A., Jesmanowicz, A., Wong, E. C. and Hyde, J. S. Processing strategies for time-course data sets in functional MRI of the human brain. *Magn. Reson. Med.* **30**, 161–173 (1993).
30. Forman, S. D., Cohen, J. D., Fitzgerald, M., Eddy, W. F., Mintun, M. A. and Noll, D. C. Improved assessment of significant activation in functional magnetic resonance imaging (fMRI): use of a cluster-size threshold. *Magn. Reson. Med.* **33**, 636–647 (1995).
31. Johnson, P. C. *Peripheral Circulation.* Wiley, New York (1978).
32. van As, H., and Schaaffsma, T. J. Flow in nuclear magnetic resonance imaging. In *Introduction to Biomedical Nuclear Magnetic Resonance* ed by S. B. Petersen, R. N. Muller and P. A. Rinck, ch. 11, pp. 68–95. George Theme, New York (1985).
33. Lai, S., Haacke, E. M., Reichenbach, J. R., Kuppusamy, K., Hoogenraad, F., Takeichi, H. and Lin, W. *In vitro* quantification of brain activation-induced change in cerebral blood oxygen saturation using MRI. *Proceedings of the 4th Meeting of the Society of Magnetic Resonance*, p. 1756 (1996).
34. Kim, S.-G. and Ugurbil, K. Comparison of blood oxygenation and cerebral blood flow effects in fMRI: estimation of relative oxygen consumption change. *Magn. Reson. Med.* **38**, 59–65 (1997).

© 1997 John Wiley & Sons, Ltd.

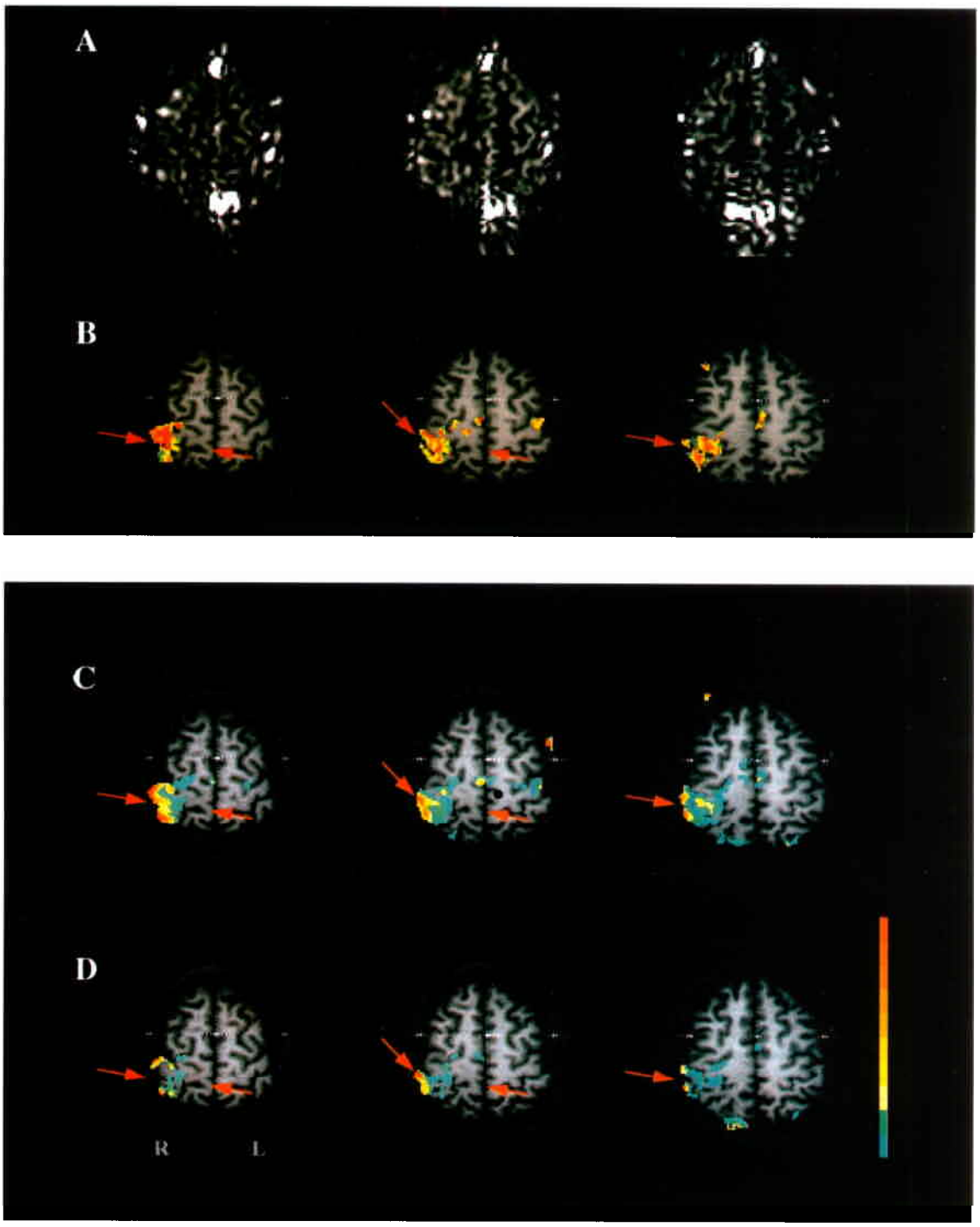

Plate 1. Representative three-slice FAIR image (A) and corresponding functional maps (B-D) overlaid on T_1-weighted EPI acquired from a subject during left-hand finger opposition. B, C and D represent functional maps based on FAIR, slice-selective IR, and nonslice selective IR, respectively. For the FAIR image, each color increment represents 10% increase of relative FAIR signal change starting from 10%, while, for nsIR images and ssIR images, each color represents a 1% increment starting from the bottom 1%. Arrows indicate the right central sulcus, and R and L refer to the right and left hemisphere, respectively. The top of the image corresponds to the anterior aspect of the brain. Note that DC offset artifacts are observed at the center of anatomical images.